

THIN FILM EFFECTS IN ULTRASONIC WAFER THERMOMETRY

F. L. Degertekin, J. Pei, B. V. Honein, B. T. Khuri-Yakub and K. C. Saraswat*

E. L. Ginzton Laboratory, Stanford University, Stanford CA 94305

*Center for Integrated Systems, Stanford University, Stanford CA 94305

ABSTRACT

Temperature is a critical parameter to be monitored and controlled in semiconductor processing. We use an ultrasonic technique where the temperature dependence of lowest order anti-symmetric Lamb wave velocity in the silicon wafer is utilized for *in-situ* temperature measurement in the 20 - 1000°C range. In almost all wafer processing steps, one or more layers of thin films are present on the wafers. The effects of these films on temperature sensitivity is investigated theoretically and experimentally. A theoretical model for Lamb wave propagation in general multilayered plates is developed using the surface impedance approach. This model is utilized to calculate the effects of anisotropy and thin films on temperature coefficients in semiconductor wafers. Calculations predict $2.38E-5$ (1°C) sensitivity for 10 cm (100) silicon wafer with 23% anisotropy. The same figures for gallium arsenide are $2.2E-5$ (1°C) and 8.7%. Thin film effects are considered for various materials commonly used in semiconductor processing. The density and shear elastic constants of film materials are found to be effective parameters in determining sensitivity figures. The frequency dependent sensitivity calculations show that it is possible to minimize effects of aluminum and silicon dioxide on silicon wafers by choosing the frequency-thickness products around 1.6 MHz-mm and 3.3 MHz-mm in temperature measurements, respectively. Using a simple propagation model, the time of flight sensitivity is also calculated and very good agreement is observed with experimental data obtained from a Rapid Thermal Processor.

INTRODUCTION

The ultrasonic wafer thermometry was introduced earlier as a new method having some advantages over existing techniques [1] [2]. The schematic diagram for ultrasonic thermometry is shown in Fig. 1. The lowest order antisymmetric Lamb waves (A0 mode) are generated and detected by PZT-5H transducers bonded to the quartz support pins. The quartz support pins are used to guide extensional waves which couple to the A0 mode in the wafer at the Hertzian contact formed at the quartz pin - wafer interface. The tips of the quartz pins are rounded and polished to have a repeatable contact. The average wafer temperature along the path joining the transmitter and receiver is inferred from the time of flight measurement. Using a precision time interval counter, the time delay between a zero crossing in the echo signal coming from the tip of the transmitter and a particular zero crossing in the received signal is measured. Since the velocity of A0 mode is

temperature dependent through the elastic constants of the wafer material, the time delay can be used to measure the temperature *in-situ* during many different semiconductor processing steps.

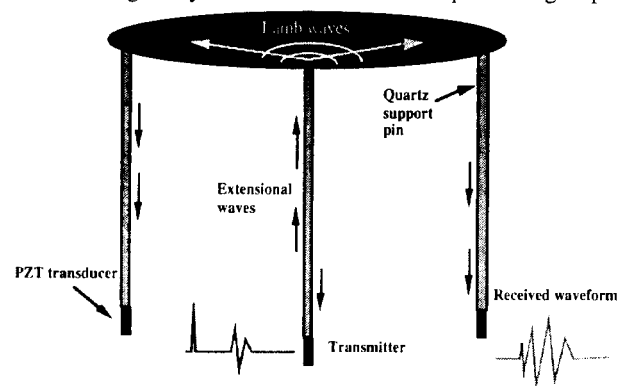


Figure 1. Schematic diagram for ultrasonic thermometry using lowest order anti symmetric Lamb waves.

One of the main advantages of ultrasonic thermometry over optical techniques such as pyrometry or ellipsometry is that the ultrasonic waves are not very sensitive to thin films on wafers. This is an important property since different kinds of thin films exist or are grown on the wafer during most of the semiconductor processes. The techniques using pyrometry depend heavily on the emissivity which is a strong function of the films on the wafer [3]. Ellipsometers can only be used with transparent films on wafers, making them unsuitable for measurements with metal films [4]. The purpose of this paper is to investigate the effects of thin films and anisotropy of semiconductor wafers on ultrasonic thermometry in general. A theoretical methodology using the surface impedance approach for Lamb wave propagation calculation in anisotropic layered plates is presented. The calculations using this model is used to predict the temperature sensitivity of the ultrasonic thermometry in presence of various thin films on the wafer. Frequency dependence of the sensitivity figures are also discussed and used to minimize the influence of thin films. The results are then compared with experimental data obtained in a rapid thermal processor.

LAMB WAVE DISPERSION CALCULATION USING THE SURFACE IMPEDANCE CONCEPT

In order to find the temperature sensitivity of A0 mode in a multilayered anisotropic plate, the dispersion curves relating the phase velocity of propagation to the frequency should be calculated. For this purpose, a model using the surface

impedance concept is developed [5] [6]. This approach eliminates the large boundary condition matrices when the partial wave approach is used to calculate propagation characteristics especially for multilayered media. Also by separating the upward and downward propagating waves during calculations, the numerical problems encountered in transfer matrix formulations are prevented. In this paper, only the definition of the global impedance tensor and the algorithm used to calculate the dispersion curves for Lamb waves are discussed. Further details of the surface impedance approach can be found in references [5] and [6].

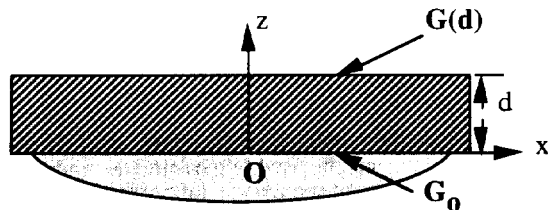


Figure 2. The geometry for surface impedance concept.

The surface impedance tensor relates the traction on a surface to the particle velocity resulting from this traction. Using the abbreviated notation [7], the traction vector \mathbf{f} on a surface normal to the z -axis and the particle velocity vector \mathbf{v} can be written as,

$$\mathbf{f} = \begin{bmatrix} T_5 \\ T_4 \\ T_3 \end{bmatrix}, \quad \mathbf{v} = \begin{bmatrix} v_x \\ v_y \\ v_z \end{bmatrix} \quad (1)$$

In case of an anisotropic layer with a surface normal to the z -axis as shown in Fig. 2, at a plane of depth z we have the equation

$$\mathbf{f}(z) = \mathbf{G}(z)\mathbf{v}(z) \quad (2)$$

where $\mathbf{G}(z)$ is defined as the global impedance tensor[6]. The surface impedance at the top of the structure shown is simply $\mathbf{G}(d)$. If we assume that the underlying medium is characterized by surface impedance \mathbf{G}_0 , so that the relation

$$\mathbf{f}(0^-) = \mathbf{G}_0\mathbf{v}(0^-) \quad (3)$$

holds, assuming plane harmonic waves with $e^{i\omega t}$ time variation, we can write the equation for $\mathbf{G}(d)$ as

$$\mathbf{G}(d) = h(\mathbf{C}, \mathbf{G}_0, \omega, k_x, d) \quad (4)$$

where \mathbf{C} , ω , k_x are elastic stiffness matrix of the layer material, angular frequency and the wave number in x direction, respectively. The function h can be considered as an impedance transformation that relates the impedance at a certain depth in layer medium to the surface impedance seen at the interface between the underlying medium. Using equation 4 recursively, the surface impedance of multilayered anisotropic media can be found. The propagation characteristics can then be obtained by imposing appropriate boundary conditions. The evaluation of impedance transformation for each layer involves an eigensystem solution of a (6x6) real matrix, and inversion of (3x3) matrices, none of which presents any numerical problems [6].

For Lamb wave propagation calculations, a multilayered anisotropic plate with N layers is assumed with the i^{th} layer

having a thickness d_i as in Fig. 3. Traction free boundary conditions are imposed at the top and bottom surfaces of the plate. With these assumptions, the following algorithm is used to calculate the phase velocity of Lamb waves as a function of frequency:

1. Assuming traction free bottom surface set $\mathbf{G}_0=0$.
2. Rotate elastic stiffness matrices to desired orientation using Bond transformations.
3. Assign the frequency and phase velocity in x -direction, i.e. set ω and k_x ..
4. Recursively calculate the surface impedance at the top surface using equation 4,

$$\mathbf{G}_i \left(\sum_{k=1}^i d_k \right) = h(\mathbf{C}_i, \mathbf{G}_{i-1}, \omega, k_x, d_i) \quad (5)$$

to find $\mathbf{G}_{\text{top}} = \mathbf{G}_N(d_{\text{tot}})$, where $d_{\text{tot}} = \sum_{k=1}^N d_k$.

5. Since the top surface is traction free, the equation

$$\mathbf{f}(d_{\text{tot}}) = \mathbf{G}_{\text{top}} \mathbf{v}(d_{\text{tot}}) = 0 \quad (6)$$

should be satisfied. To have a non zero particle velocity, the determinant of surface impedance at the top surface should vanish, so check the condition

$$\det \mathbf{G}_{\text{top}} = 0 \quad (7)$$

If equation 7 is satisfied, the phase velocity at given frequency is found. Otherwise go to step 3, and iterate.

The above algorithm is used with a fast converging search method to calculate the phase velocity of Lamb waves in general multilayered anisotropic plates.

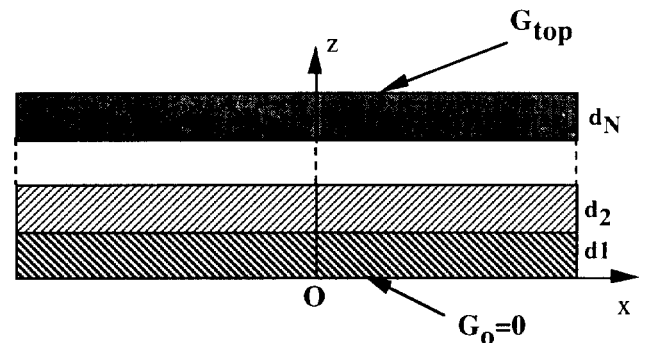


Figure 3. Geometry and coordinates for multilayered anisotropic free plate.

THEORETICAL RESULTS

Temperature sensitivity of plain semiconductor wafers

The effect of temperature on the phase velocity of Lamb waves is included in calculations using the published temperature coefficients for elastic constant [8] [9]. Fig. 4 depicts the absolute calculated temperature sensitivity of phase velocity (dv/vdT) of A0 mode for silicon and gallium arsenide as a function of frequency thickness product (fd) in the typical range of ultrasonic thermometry. Direction of propagation is $\langle 100 \rangle$ in a (100) oriented wafer. Temperature sensitivity increases with frequency for both materials. For $fd \sim 0.1$ MHz-mm corresponding to a 0.5 mm wafer with 200 kHz operation frequency, the sensitivity is around $-2.38E-5$ ($1/^\circ\text{C}$) for silicon

and -2.23×10^{-5} ($1/^\circ\text{C}$) for gallium arsenide. Both figures are more than an order of magnitude higher than the corresponding thermal expansion coefficients.

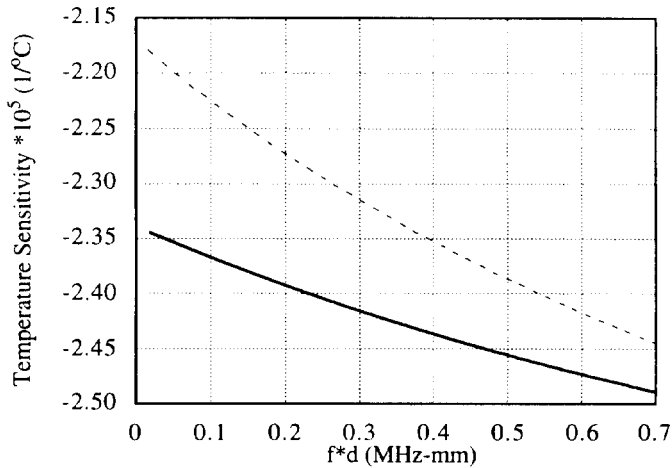


Figure 4. Temperature sensitivity of A0 mode phase velocity variation in $\langle 100 \rangle$ direction as a function of frequency thickness product. Calculated data for (100) silicon (solid line) and gallium arsenide (dashed line) wafers.

Fig. 5 depicts the variation of temperature sensitivity as a function of propagation direction for (100) wafers at $fd = 0.1$ MHz-mm, which corresponds to a sensor operating around 200 kHz on a standard 10 cm diameter wafer. The 4-fold symmetry of this plane is clearly seen in sensitivity results and the variation is around 22% for silicon and 8.7% for gallium arsenide. The sensitivity is maximum and the rate of change is minimum in $\langle 100 \rangle$ direction, pointing to the advantages of this particular direction for temperature measurement in terms of signal-to-noise and alignment tolerance.

Effect of thin films

When one or more thin layers are deposited at the surface of a relatively thick plate, the phase velocity of Lamb waves is affected depending on the material properties of the layers and plate. It is possible to exploit this sensitivity to measure thickness and properties of thin films. The algorithm described in the previous section is used to calculate phase velocity of A0 mode for common thin film structures used in semiconductor processes. Fig. 6 shows the phase velocity variation of the A0 mode in a 0.5 mm (100) silicon wafer at 200 kHz with film thickness for different kinds of films. The variation is linear in this film thickness range, since the film is a small perturbation on the silicon plate. For aluminum and silicon dioxide, which have densities close to silicon and lower shear constant c_{44} , the phase velocity has a positive slope with the film thickness. For silicon nitride, which is harder than silicon, the slope is $2.8\text{m/sec}/\mu\text{m}$ indicating the stiffening effect. In the case of copper, the variation has a slope of $-0.6\text{m/sec}/\mu\text{m}$ due to the loading caused by high density. The results indicate that the relative density and shear elastic constant c_{44} of the films dominate the variation of phase velocity in this range. This can be attributed to the shear nature of A0 mode, which is predominantly a flexural wave.

The variation of absolute phase velocity sensitivity as a function of fd is plotted in Fig. 7 with d being the thickness of the silicon plate. Different kinds of films are also considered for these

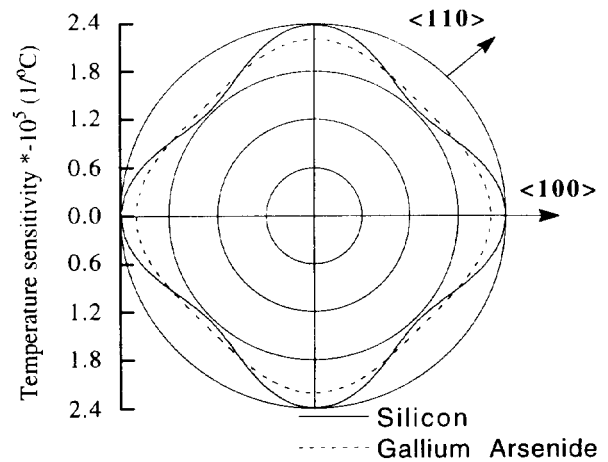


Figure 5. Variation of phase velocity temperature coefficient (dv/vdT), with direction for (100) gallium arsenide and silicon wafers ($fd = 0.1$ MHz-mm)

calculations. For aluminum and silicon dioxide, a zero crossing in sensitivity occurs around $fd = 1.6$ and $fd = 3.3$ MHz-mm, respectively. At the low frequency regime, these films have the effect of increasing plate thickness resulting the positive sensitivity due to dispersion. As the frequency increases more energy is concentrated at the surface and the slower surface wave velocity of the films begin to force the sensitivity to be negative as expected from perturbation theory [7]. These curves can be used to minimize the velocity variations due to thin films having proper elastic constants during temperature measurement. Noting the weak dependence of temperature

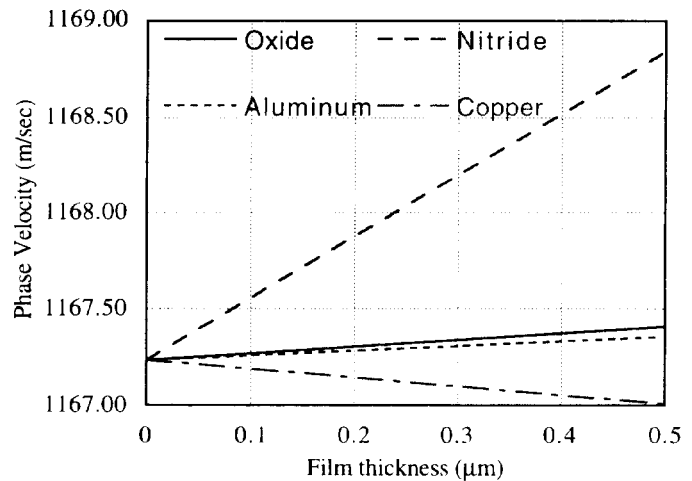


Figure 6. Calculated phase velocity variation of A0 mode with different film materials. The silicon wafer is 0.5 mm thick and $f=200$ kHz.

sensitivity to frequency as depicted in Fig. 4, and using two different frequencies for ultrasonic time of flight measurement simultaneously, it is possible to decouple the effects of thin film growth and temperature leading to *in-situ* measurement of both parameters during semiconductor processing.

For ultrasonic thermometry, the velocity variation due to thin films causes an absolute change in time of flight at constant temperature which can be predicted using the model developed. The other effect that should be considered is the temperature sensitivity variation in the presence or during growth of thin

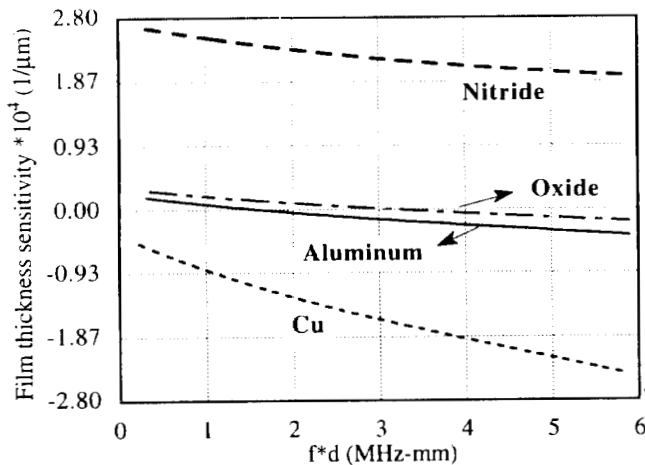


Figure 7. Calculated film thickness sensitivity of A0 mode as a function of frequency-thickness product for different materials on silicon wafer.

films. To predict these effects, the elastic constants of thin films are also varied with temperature in calculations. The results for silicon dioxide and aluminum on (100) silicon in <100> direction are depicted in Fig. 8 for $fd = 0.1$ MHz-mm. These materials are chosen for their importance in semiconductor processing. Temperature sensitivity of phase velocity decreases 0.96% for 1 μm silicon dioxide whereas for aluminum of the same thickness, it changes 1.2% in the opposite direction. These values can be attributed to the relative temperature coefficients of the film materials. The results show that the cross coupling between the thin film effects and temperature is not very critical. For practical cases such as very thin gate oxide growth with oxide thickness in the range of 100-200 \AA , the effect of the film can be neglected even for accuracy around $\pm 1^\circ\text{C}$.

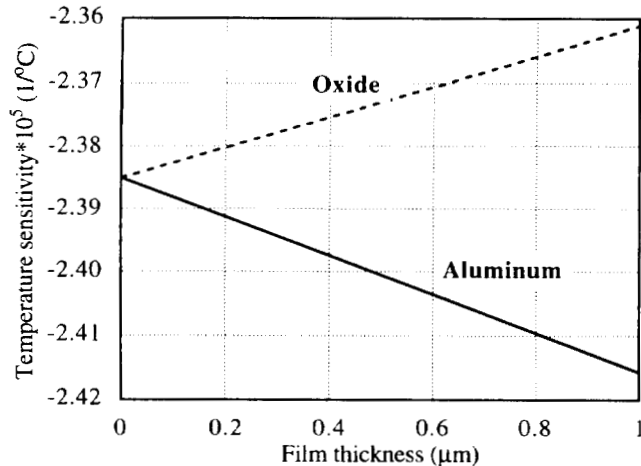


Figure 8. Temperature sensitivity of A0 mode phase velocity as function of film thickness. $fd = 0.1$ MHz-mm, (100) silicon in <100> direction

EXPERIMENTAL RESULTS

The temperature sensitivity figures for Lamb wave velocity calculated in previous sections do not provide the information for direct comparison of theory and experiments in ultrasonic thermometry. Since for temperature measurement, a pulse is applied to the PZT transducer rather than a CW signal, the

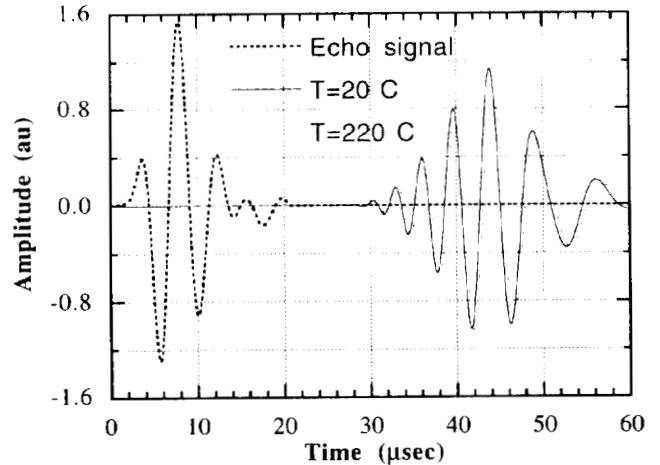


Figure 9. The experimental echo signal and calculated output waveforms at wafer temperatures $T=20^\circ\text{C}$ and $T=220^\circ\text{C}$. The pin to pin spacing is 83.4 mm.

effect of finite bandwidth should be considered. Also, particular zero crossings in the echo and received signal should be tracked as in the experiments. For this purpose, the experimental echo signal is used as the input for theoretical calculations. This pulse, which is depicted in Fig. 9, is propagated through the wafer using the calculated dispersion curves assuming a point source excitation. The result of this calculation for a 0.5 mm thick (100) silicon wafer at $T=20^\circ\text{C}$ and $T=220^\circ\text{C}$ are shown also in Fig. 9 for a pin to pin spacing of 83.4 mm. The temperature change results in a shift in time for the received waveform zero crossing determined by the dispersion curve. The calculations show that this shift is a linear function of the wafer temperature.

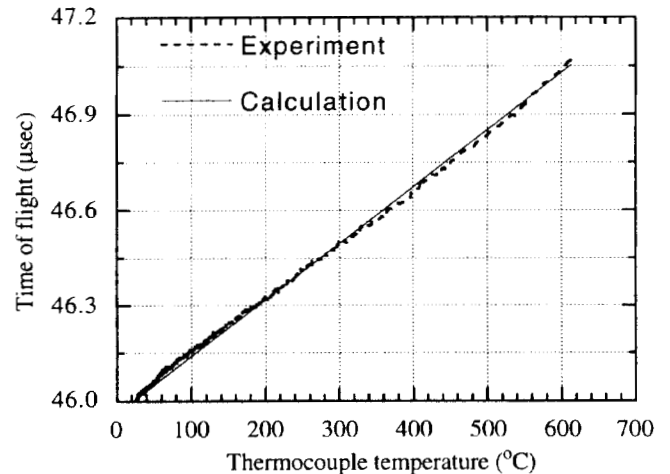


Figure 10. Experimental and calculated time of flight data vs. thermocouple temperature obtained by tracking a particular zero crossing in a Rapid Thermal Processor.

In Fig. 10, the experimental data obtained from a rapid thermal processor is compared with theory. In this case a later zero crossing is tracked for time of flight measurement resulting the time delay around 46 μsec between the zero crossings. The calculations predict a 1.78 $\text{nsec}/^\circ\text{C}$ sensitivity for time of flight, which is plotted as the solid line. The phase differences which occur due to signal conditioning circuitry used in experiments is accounted for by adding a shift to the theoretical time delay. The effect of thermal expansion is also taken into account in the calculations. With these considerations, the agreement with

theory is very good, showing the validity of temperature coefficients, but further measurements for variation of temperature coefficients with temperature should be made for better agreement and absolute measurements.

CONCLUSION

A theoretical model based on the surface impedance concept is developed to investigate Lamb wave propagation in general anisotropic layered plates. This model is used to calculate the effects of temperature, thin films and their combined influence on phase velocity. The results indicate that for some film materials such as silicon dioxide and aluminum, the phase velocity sensitivity can be minimized by particular choice of frequency for temperature measurement. Also, for processes involving very thin films in the order of 100-200 Å thickness, the overall effect of the films can be neglected for temperature accuracy in the range of $\pm 1^\circ\text{C}$. Using a simple model for the ultrasonic thermometry system, the experimental results are predicted with high accuracy. It is possible to extend these results to apply to more complicated ultrasonic temperature measurement problems such as temperature tomography.

ACKNOWLEDGMENTS

This work is supported by SRC under the contract no: 94-YC-704 and Sematech.

REFERENCES

- [1] Y.J. Lee, "Temperature measurement in rapid thermal processing using acoustic techniques", Ph.D. thesis, Stanford University, 1993.
- [2] F. L. Degertekin, Y.J. Lee, J. Pei, B.T. Khuri-Yakub and K.C. Saraswat, "In-situ ultrasonic thermometry of semiconductor wafers", in *Proceedings of 1993 IEEE Ultrasonics Symposium*, 1993.
- [3] P.J. Timans, "Emissivity of silicon at elevated temperatures", *J. Appl. Phys.*, Vol. 74, pp. 6353-6363, November 1993.
- [4] R.K. Sampson, K.A. Conrad, E.A. Irene and H.Z. Massoud, "Simultaneous Silicon wafer temperature and oxide film thickness in rapid thermal processing using ellipsometry", *J. Electrochem. Soc.*, vol. 140, no. 6, pp. 1734-1743, June 1993.
- [5] A.M. Braga and G. Herrmann, "Plane waves in anisotropic layered composites", in *Wave propagation in Structural Composites*, A.K. Mal and T.C.T. Ting, ed. New York: ASME-AMD Vol. 90, pp. 81-98 1990.
- [6] B. Honein, A.M. Braga, P. Barbone and G. Herrmann, "Wave propagation in piezoelectric layered media with some applications", *Journal of Intelligent Material Systems and Structures*, Vol. 2, pp. 542-557, 1992.
- [7] B.A. Auld, *Acoustic fields and waves in solids*, New York: John Wiley & Sons Inc., Vol. 1&2, 1973.
- [8] H.J. McSkimmin, W.L. Bond, E. Buehler and G.K. Teal "Measurement of the elastic constants of silicon single crystals and their thermal coefficients", *Phys. Rev.*, Vol. 83, p 1080, 1951.
- [9] G. Simmons and H. Wang, *Single crystal elastic constants and calculated aggregate properties: a handbook*, Cambridge: The MIT press, 1971.

